Photopolymerization Kinetics and Structure Development of Templated Lyotropic Liquid Crystalline Systems

Christopher L. Lester, Colleen D. Colson, and C. Allan Guymon*

Department of Polymer Science, University of Southern Mississippi, Hattiesburg, Mississippi 39406-0076

Received October 27, 2000; Revised Manuscript Received March 12, 2001

ABSTRACT: The templating of the ordered nanostructures of lyotropic liquid crystals (LLC) onto organic polymers has recently been of great interest. This work describes the polymerization and segregation behavior of polar and nonpolar monomers in an LLC environment. Nonpolar monomers partition to the oil-soluble domains of the LLC phase, whereas more polar monomers segregate at the interface of the liquid crystals. The polymerization kinetics in both cases are significantly influenced by the LLC phase morphologies although in different ways. The nonpolar monomers exhibit the fastest polymerization rates in micellar aggregates. This behavior is a result of an increase in the rate of propagation, induced by higher local concentrations of monomer in the micelles as compared to other mesophases. For more polar monomers, the opposite polymerization behavior is observed. The fastest polymerizations for these monomers are observed in the highly ordered lamellar mesophase with the minimum polymerization rate observed in the isotropic micellar phase. In this case, the enhanced polymerization rates are a consequence of depressed termination rates. This decrease in termination rate is due to diffusional limitations induced by the high degree of order in a lamellar mesophase. Initial results also indicate that the original LLC phase morphologies are retained after photopolymerization.

Introduction

Lyotropic liquid crystals (LLC) possess highly ordered nanostructures that have been of great interest for a number of years from both a fundamental and applied standpoint. Because LLC phases lack the necessary physical robustness for a number of applications, templating the LLC phase morphology onto other materials including organic polymers has also been proposed. Applications such as membranes, separation devices, and drug delivery devices are only a few examples in which it would be desirable to have a controlled polymer nanomorphology. However, considerable difficulties arise in templating LLC structures onto organic polymers. It is entropically unfavorable for polymers to exist in the confined dimensions of LLC phases, and often phase separation occurs. Often the types of morphologies generated are indeed nanoporous but not the same as the original LLC structure and are products of phase separation phenomenon.[1,2] The ability to generate organic polymers with templated LLC phase structure would be of great value in a wide variety of applications.

LLC phases usually consist of an amphiphile and a typically aqueous solvent. At sufficient concentrations of amphiphile with appropriate molecular geometry, a variety of ordered structures are formed. At low amphiphile concentrations, spherical micelles appear. With successive increases in amphiphile concentration, the morphologies of the aggregates change to rodlike structures packed into hexagonal arrays and bilayer aggregates that are referred to as lamellar mesophases. Other LLC phases that may also include bicontinuous and discontinuous cubic arrays of surfactant aggregates.[3−5] A particularly interesting feature of LLCs is that they possess a nanometer size scale making them useful for a number of applications. Additionally, the unique ordering characteristics provided by these materials may facilitate the understanding of the effect of nanoscale order on reaction kinetics.

Reactions in ordered media have proven to behave significantly different than in an isotropic state. These reactions are highly dependent on the type and degree of order in a given system. For example, the polymerization kinetics of a variety of monomers in small molecular mass thermotropic liquid crystals change dramatically when performed in the different liquid crystalline phases. Polymerization rates more than double at lower temperatures, corresponding to layered smectic phases.[6,7] This phenomenon can be attributed to a number of factors including diffusional limitations that reduce termination rates and segregation of the monomeric species that increases both the apparent propagation and termination values.[8] Additionally, the polymerization behavior and segregation of various monomers in thermotropic liquid crystalline solvents dramatically impact the electrooptic and optical properties when prepared under different conditions.[9] These studies have helped elucidate the polymerization kinetics in organized media and the impact of polymerization behavior on ultimate properties of polymer/liquid crystalline composites. Similar studies examining polymerizations in lyotropic systems could give significant information both on the formation of lyotropic liquid crystalline order in polymers and on the retention of structure for selected applications.

One route to synthesizing polymers with LLC order is by synthesizing monomers that are, in and of themselves, amphiphilic. Previous work in this area has yielded mixed results as lyotropic structures are not typically retained or are significantly altered upon polymerization.[10−14] On the other hand, a limited number of cases have been reported showing retained LLC structure upon polymerization. For example, O'Brien et al. polymerized a dienoyl phospholipid in the inverted hexagonal phase with retention of the original lyotropic

* To whom correspondence should be addressed.

10.1021/ma001853e CCC: $20.00
Published on Web 05/03/2001

structure.[15] The original lyotropic structure of other dienoyl-substituted phospholipids that exhibited the bicontinuous cubic and inverted hexagonal phases has also been successfully retained.[16] Other monomers exhibiting the inverse hexagonal phase have been stabilized through polymerization by Gin et al. for potential application in nanocomposite synthesis and for novel organic catalysis.[17−19] However, the impact that these ordered arrays have on the polymerization kinetics has not been adequately addressed, and conversely, the relationship between polymerization kinetics and structure retention requires more attention. Recently, the polymerization kinetics of ordered assemblies of a semifluorinated polymerizable LLC have been studied. The type and degree of lyotropic structure play a significant role in the polymerization rate. The more ordered lamellar phases exhibit faster polymerization rates, and with decreasing degree of lyotropic order the polymerization rate consequently decreases. The rate enhancements are a result of the highly ordered system imposing diffusional limitations on the growing polymer which yields a slower termination rate. Enhanced structure retention was correlated with faster polymerization rates, implying that kinetics are a major factor in retaining the original LLC phase structure.[20]

Synthesis of nanoporous materials has also been investigated by solvating precursor materials in surfactant/water mixtures or block copolymers with subsequent polymerization. Successful templating has been observed with a variety of inorganic materials such as silicates and cadmium compounds.[21−27] The polymerization of a variety of conventional organic monomers solvated in LLC media has also been attempted in order to develop the unique LLC polymer nanostructure in these systems. This research has seen limited success in templating the actual lyotropic structure onto polymeric materials. The polymerization of a water-soluble monomer in the bicontinuous cubic phase of a cationic surfactant, for example, has been reported in which the triply periodic nanostructure was templated onto the polymer.[28] Additionally, two different polymerizable amphiphiles have been used with polar and nonpolar comonomers to formulate bicontinuous cubic phases, which form periodic nanoporous gels upon polymerization.[29]

Templating the LLC phase onto an organic polymer system has proven difficult in most cases, however, and typically yields nanostructures that result from phase separation and not from the liquid crystalline arrays. In fact, polymerization kinetics have been implicated as being the controlling factor in the types of morphologies generated, but little information regarding the kinetics is available.[2,30] Consequently, polymerization behavior in LLC media needs to be more fully understood in order to successfully generate nanostructured polymers that are a result of the original lyotropic structure. It is therefore important to determine the role that LLC phase structures plays in the polymerization mechanism of a variety of monomers and conversely the effect that the polymerization has on the resulting polymer structure to allow control and development of LLC phase structure in templated polymerizations.

The polymerization kinetics and consequently the ultimate order of the polymer formed in the LLC aggregates will depend significantly on the different types of ordered phases assumed. Conversely, the overall structure of the resulting material will strongly be affected by the polymerization behavior. The goal of this work is to examine the polymerization kinetics of a variety of monomers segregated in the LLC phases of a common surfactant. The polymerization kinetics and phase behavior under a variety of conditions will be correlated so that favorable morphologies for a variety of applications may be obtained. Monomers of different polarities will be utilized to determine how the different regions of the LLC affect the polymerization and to determine which domains are more resilient to the evolving polymer. Both monofunctional and difunctional monomers will be examined to determine the impact of cross-linking on structure retention. After incorporating these monomers into varying compositions of surfactant and water, any changes in the phase behavior will also be observed. A systematic study examining the polymerization kinetics of these monomers sequestered in LLC phases will elucidate details about the effect of ordering on the polymerization mechanism and facilitate optimization of conditions for retention of structure. An understanding of these effects will greatly facilitate the development of nanostructured polymers for a variety of different applications including tissue scaffolding, delivery systems for oil-soluble materials, and media for membrane-mediated chemistries.

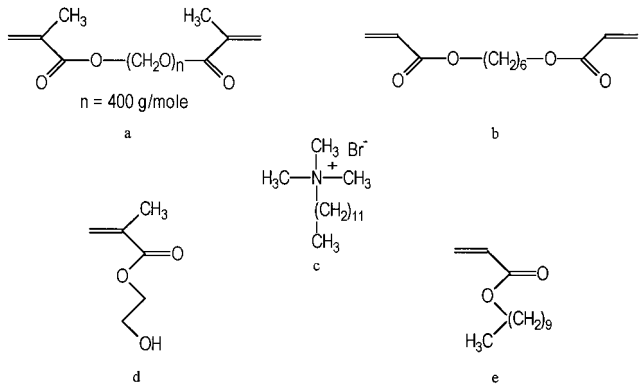

Figure 1. Chemical structure of monomers and surfactant used in this study. Shown are (a) poly(ethylene glycol)-400 dimethacrylate (PEG-400-DMA), (b) hexanediol diacrylate (HDDA), (c) dodecyltrimethylammonium bromide (DTAB), (d) 2-hydroxyethyl methacrylate (HEMA), and (e) *n*-decyl acrylate (*n*-DA).

Experimental Section

Nonpolar diacrylate monomers used in this study are hexanediol diacrylate (HDDA, Polysciences) and *n*-decyl acrylate (nDA, Polysciences.) The polar monomers used include poly(ethylene glycol)-400 dimethacrylate (PEG 400-DMA, Aldrich) and 2-hydroxyethyl methacrylate (HEMA, Aldrich). Dodecyltrimethylammonium bromide (DTAB, Aldrich) and deionized water comprise the LLC system. The chemical structure of these compounds is shown in Figure 1. The photopolymerizations were initiated using Irgacure 2959 and Irgacure 651 (Ciba Specialty Chemicals, Tarrytown, NY). Approximately 1 wt % initiator with respect to the total monomer weight was incorporated into the LLC samples.

Procedure. Small-angle X-ray scattering (SAXS) was used to characterize the phase behavior using a Siemens XPD 700P WAXD/SAXS with a Cu Kα line of 1.54 Å. Bragg's law was used to determine the *d* spacing of the lyotropic mesophase both before and after polymerization. Confirmation of phase type was obtained through the characteristic ratios of the higher order peaks.[3] A polarized light microscope (Nikon, Optiphot-2 pol) equipped with a hot stage (Instec, Boulder, CO) was utilized to corroborate data collected with SAXS by looking for characteristic textures of the various mesophases as well as phase transitions.

Reaction profiles were monitored in real time with a differential scanning calorimeter (Perkin-Elmer DSC-7) modified with a medium-pressure UV arc lamp and quartz windows. Samples were covered with a thin film of FEP (DuPont fluorinated copolymer) to prevent evaporation of water. The DSC sample cell was also attached to a refrigerated circulating chiller (VWR Scientific Products-1150A) to maintain isothermal reaction conditions. The DSC cell was purged with nitrogen for 10 min prior to exposing the sample to the UV light source in order to prevent oxygen inhibition during the polymerization. The samples were also heated to 80 °C and cooled to 30 °C at 10 °C/min to ensure uniform thickness and good thermal contact. The polymerizations were initiated with monochromatic 365 nm light at an intensity of 4.5 mW/cm^2.

The heat of polymerization was utilized to directly calculate the rate of polymerization. For these studies the theoretical values of 20.6 and 13.1 kcal/mol were used as the heat evolved per acrylate and methacrylate double bond reacted, respectively.[31] Maximum rates were taken from the peak of the rate profiles obtained.[32] To determine individual rate parameters of termination and propagation, a series of after-effect experiments were performed. First, a lumped kinetic constant $k_p/k_t^{1/2}$ was measured as a function of time from the steady-state polymerization rate profile. By closing a light shutter between the UV light source and the sample at various times during the polymerization process, the initiation step is eliminated. The propagation and termination rate parameters can then be decoupled. This method of determining individual rate parameters is described in detail elsewhere.[8]

Results and Discussion

Polymers with morphologies on the nanometer size scale would be beneficial for many applications such as catalytic media, nanocomposite synthesis, and biomimetic materials. Templating LLC phase structure onto organic polymers is an ideal route to such materials. This templating has proven difficult, yielding materials with morphologies that are typically a result of phase separation. As stated previously, the goals of this work are to yield a better understanding of the polymerization kinetics in lyotropic liquid crystals and to determine the impact that the LLC phase morphology and polymerization kinetics have on the resulting polymer. These research goals consequently require the selection of a LLC system that displays a variety of lyotropic morphologies. The DTAB/water system is ideal as it possesses three distinct LLC morphologies. At concentrations above 40 wt % in water, DTAB aggregates into micelles and with successive increases in concentration the discontinuous cubic, hexagonal, and lamellar phases are formed.[33] After incorporation of significant amounts of monomer, the phase behavior changes slightly, but the three liquid crystalline phases of interest are still exhibited as confirmed with polarized light microscopy and SAXS. As can be seen in Figure 2, the d_{100} spacings calculated from the primary SAXS reflections also change with incorporation of monomer. These *d* spacings are plotted as a function of surfactant/water weight ratio. The addition of the oil-soluble monomer HDDA causes the *d* spacings to increase slightly over all compositions, indicating that the hydrocarbon domains of the lyotropic structures are being swollen with monomer. With the addition of the water-soluble monomers PEG-400-DMA and HEMA, the opposite phenomenon is observed in that a contraction of the *d* spacings occurs. This contraction of *d* spacing is due to the monomers shielding the ionic headgroups of the surfactant from one another. This shielding of the ionic headgroups allows the aggregates to more closely pack. Consequently, the monomers are either freely solvated in the water domains or possibly aggregating at the water/oil interface with the DTAB.

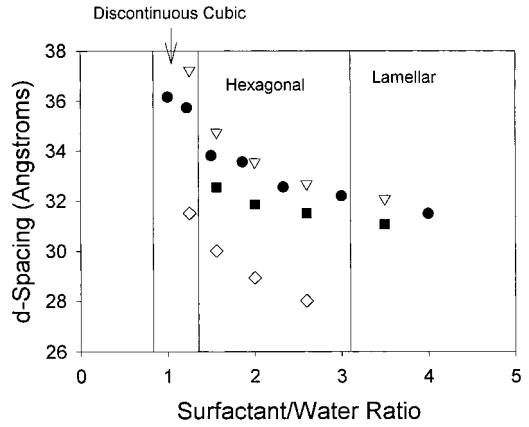

Figure 2. *d* spacing of various DTAB/water LLC systems containing 0% monomer (●), 10% HDDA (▽), 20% PEG-400-DMA (■), and 20% HEMA (◇) as a function of surfactant-to-water ratio.

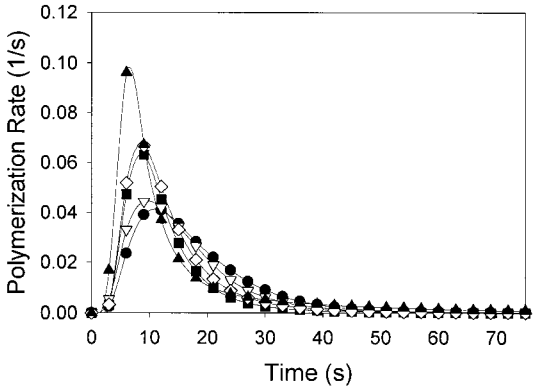

Figure 3. Polymerization rate vs time for 10 wt % HDDA in the LLC phases of DTAB/water with increasing DTAB concentration. Shown are 40% cubic (▲), 50% hexagonal (◇), 60% hexagonal (■), 70% lamellar (▽), and 80% lamellar (●) weight percent DTAB.

As mentioned previously, the primary goal of this work is to determine the effect of different LLC phase morphologies on the polymerization mechanism of a variety of monomers. Samples ranging from 35 to 70 wt % DTAB were selected as this concentration range exhibits the discontinuous cubic, hexagonal, and lamellar phases. Interestingly, the polymerization kinetics of monomers of different polarities segregated into distinct regions of the LLC phases exhibit very different polymerization behavior. In Figure 3 the polymerization rate profiles of 10% HDDA in the LLC DTAB/water system are shown as a function of time. The polymerization rate behavior is vastly different as phase behavior changes with increasing concentration of DTAB. The fastest polymerization rate is observed at 40% DTAB corresponding to a discontinuous cubic morphology. At slightly increased DTAB concentrations (50% and 60%) in the hexagonal phases, a discontinuous drop in polymerization rate is observed. Finally, after attaining the lamellar morphology at 70% and 80% DTAB, the lowest polymerization rate profiles are observed.

To illustrate this behavior in more detail, the peak polymerization rates of 10% HDDA are plotted for various concentrations of DTAB/water in Figure 4. The highest rates are observed in the discontinuous cubic liquid crystalline phase. With increasing DTAB concen-

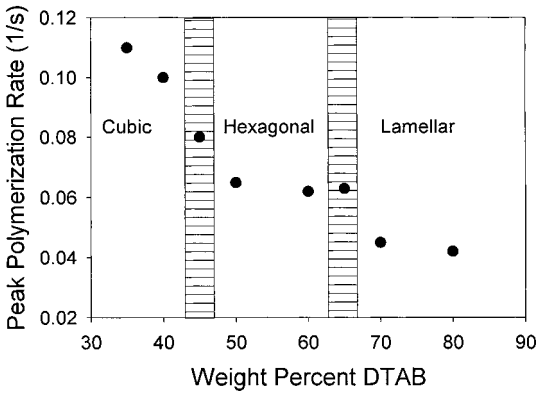

Figure 4. Peak polymerization rates of 10% HDDA in the LLC phases of DTAB/water as a function of DTAB concentration.

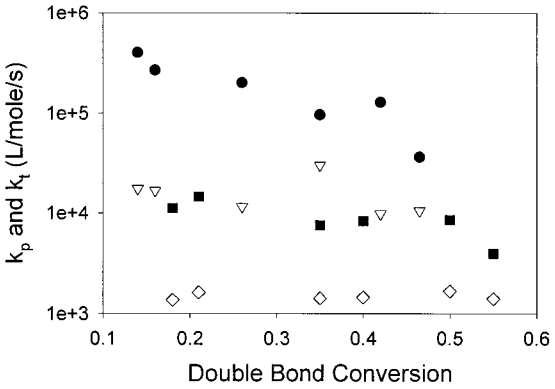

Figure 5. Termination (k_t) and propagation (k_p) rate parameters of 10% HDDA in LLC phases of DTAB/water, shown as a function of double-bond conversion. Given are k_t for 70% DTAB-lamellar (●), k_t for 40% DTAB-cubic (■), k_p for 70% DTAB-lamellar (▽), and k_p for 40% DTAB-cubic (◇).

tration a mixed phase of hexagonal and cubic morphology is obtained, and a decrease in polymerization rate is seen. At higher concentrations of DTAB the homogeneous hexagonal liquid crystalline phases, the rate decreases by more than 30%. It is important to note that the polymerization rate stays virtually the same with large increases in DTAB concentration within the hexagonal liquid crystalline phase. When polymerizing 10% HDDA in the lamellar phase of DTAB/water, a $2^1/_2$-fold decrease in the peak polymerization rate from that of the discontinuous cubic phase is evident. Interestingly, only small differences in the polymerization rate of HDDA are seen within each phase. Discontinuous decreases in the polymerization rate occur, however, with changes in LLC phase.

To explain these results, after-effect experiments were performed with the DTAB/water/HDDA system. Figure 5 depicts the apparent propagation and termination rate parameters, designated k_p and k_t, for the rapidly polymerizing discontinuous cubic sample and that of the lamellar phase that polymerizes $2^1/_2$ times slower. The k_p and k_t parameters are shown for a range of conversions. Over this range of conversions the k_p of the cubic phase is an order of magnitude higher than that of the lamellar phase which could explain the faster polymerization rate. However, a similar order of magnitude increase in k_t is observed for the cubic liquid crystalline phase, which indicates a faster rate of termination. This increase in rate of termination alone would actually lower the polymerization rate. As the polymerization rate is dependent on $k_p/k_t^{1/2}$, a similar increase of both k_p and k_t corresponds to an overall faster polymerization rate. Analogous results are observed in polymerizations of small amounts of monomer in a thermotropic liquid crystalline solvent.[8] Increases in both k_p and k_t indicate an increase in local monomer concentration which, in this case, is induced by greater segregation in the smaller micellar aggregates.

In fact, the segregation factor can be calculated by using a model developed previously.[8] The segregation factor is calculated by using eq 1.

$$\alpha = \frac{k_t}{k_t'} \tag{1}$$

In this case k_t' is the termination rate parameter for that of the cubic liquid crystalline phase consisting of 40 wt % DTAB, k_t is the rate parameter for the lamellar phase made up from 70 wt % DTAB, and α represents the segregation factor. In this case α is approximately 0.1, which means the monomer is actually 10 times more concentrated in the cubic liquid crystalline phase than in the lamellar phase. The large increases in rate can therefore be directly attributed to differences in segregation of the monomer. In the discontinuous cubic liquid crystalline phase, the surfactant concentration is significantly lower than that of the hexagonal or lamellar mesophase. This lower surfactant concentration has the effect of concentrating the monomer as it is nonpolar and has less volume in which to be solubilized. These differences in surfactant concentration alone do not adequately account for the differences in polymerization rate, however. The calculated segregation factor of 0.1 indicates a 10-fold increase in local monomer concentration, and the surfactant concentration is only doubled when comparing the cubic micellar phase to the lamellar phase. A 2-fold increase in concentration should yield only a 2-fold increase in the apparent propagation rate. The morphology of the aggregates must be playing a large role in the increase in the local concentration of monomer. It is possible in the micellar aggregates that conformational restrictions of the nonpolar tail exist due to the curvature of the interface that allows the monomer to access only the tail ends of the hydrocarbon chains, whereby in the lamellar phase the conformation of the hydrocarbon tails is such that the monomer can access a larger volume of the aggregates. SAXS supports this hypothesis, in that the smaller aggregates with lower surfactant concentrations are swollen to a greater extent than the phases at higher surfactant concentrations.

Similar experiments were performed with the monofunctional monomer *n*-DA in the various LLC phases of the DTAB/water system. Peak polymerization rates are depicted in Figure 6 with results strikingly similar to that of the HDDA. The fastest polymerizations are recorded in the isotropic micellar phase at lower concentrations of DTAB. As with HDDA when the surfactant concentration is increased and the hexagonal liquid crystalline phase is formed, the polymerization rate decreases by approximately one-third. When the lamellar phase is attained at higher surfactant concentrations, the lowest polymerization rates are observed with an overall 2-fold decrease in polymerization rate. This polymerization behavior may be again attributed to the greater segregation in the smaller micellar aggregates. As in the case of the mixtures containing HDDA, the oil-soluble *n*-DA also segregates preferentially in the

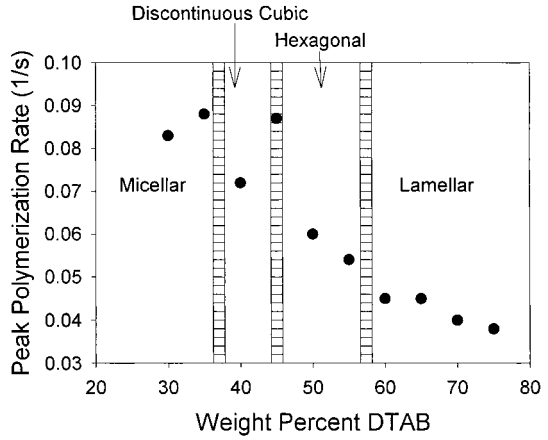

Figure 6. Maximum polymerization rates of 10% *n*-DA in the LLC phases of DTAB/water as a function of DTAB concentration.

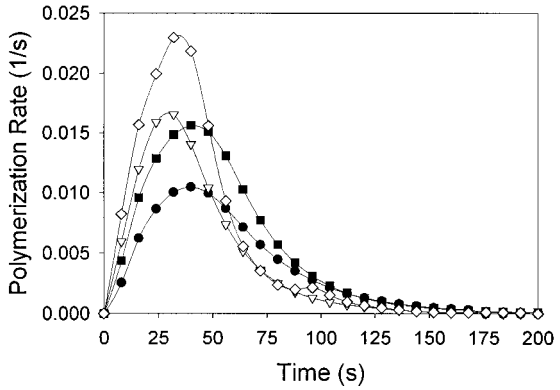

Figure 7. Polymerization rate vs time for 20 wt % PEG-400-DMA in the LLC phases of DTAB/water with increasing DTAB concentration. Shown are 35% micellar (●), 40% cubic (▽), 50% hexagonal (■), and 65% lamellar (◊) DTAB.

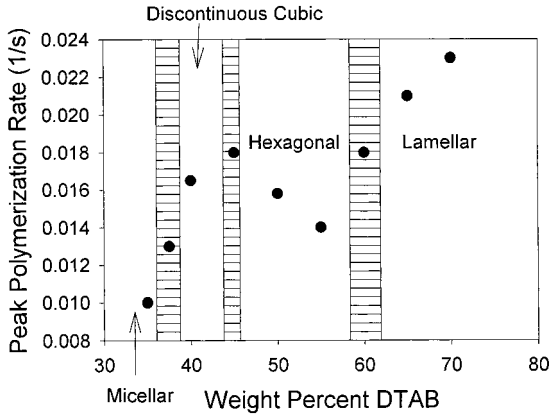

Figure 8. Peak polymerization rates of 20% PEG-400-DMA in the LLC phases of DTAB/water as a function of surfactant concentration.

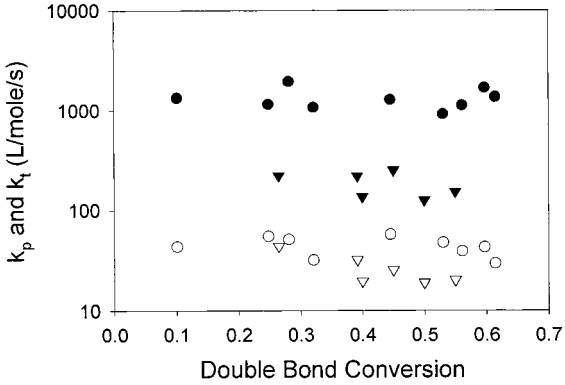

Figure 9. Termination (k_t) and propagation (k_p) rate parameters of 20% PEG-400-DMA in LLC phases of DTAB/water, shown as a function of double-bond conversion. Given are k_t for 35% DTAB-micellar (●), k_t for 70% DTAB-lamellar (▼), k_p for 35% DTAB-micellar (○), and k_p for 70% DTAB-lamellar (▽).

nonpolar domains of the aggregates. When the surfactant concentration is increased, the monomer has a greater accessible volume.

As stated previously, monomers of a more polar nature segregate to different regions of the LLC phases. Specifically, the polar monomers segregate into the aqueous domains and are likely associated closely with the polar headgroups of the surfactant at the interface. As a result of this different segregation behavior, the water-soluble monomer PEG-400-DMA exhibits vastly different polymerization behavior than the nonpolar HDDA. In Figure 7 the polymerization rate profiles of various concentrations of DTAB/water with 20% PEG-400-DMA are shown. In this case the lamellar mesophase at 70% DTAB yields the fastest polymerization rate profile. The polymerization rate decreases by approximately one-third when the DTAB concentration is decreased to produce a hexagonal liquid crystalline phase. The discontinuous cubic liquid crystalline phase at 40% DTAB exhibits a polymerization rate even higher than that of the hexagonal mesophase. The isotropic micellar phase at 35% DTAB polymerizes more than $2^1/_2$ times slower than the rapidly polymerizing lamellar phase. This decrease in polymerization rate is a result of the significantly less ordered isotropic micellar phase.

To see this behavior in more detail, the peak polymerization rates of rate profiles obtained of the various LLC samples containing 20 wt % PEG-400-DMA were plotted as a function of DTAB concentration in Figure 9. The fastest polymerization rates are observed in the lamellar samples. A mixed lamellar/hexagonal phase exists at weight percents of DTAB close to 60% and is denoted by the region of horizontal lines. The peak polymerization for this mixed phase is slightly less than that of the homogeneous lamellar mesophase. The homogeneous hexagonal phase at lower DTAB concentration has a peak polymerization rate nearly half that seen in the lamellar morphology. The polymerization rate then increases slightly with the formation of a mixed phase of hexagonal and discontinuous cubic aggregates. In the discontinuous cubic liquid crystalline phase at 40 wt % DTAB, the polymerization is slightly faster than that of the hexagonal liquid crystalline phase but is still significantly slower than that of the lamellar mesophase. After lowering the concentration further to a mixed phase consisting of isotropic micelles and discontinuous cubic liquid crystals the polymerization rate decreases to approximately half of the lamellar phase. The homogeneous isotropic micellar phase at 35 wt % DTAB exhibits the slowest polymerization rate that is approximately $2^1/_2$ times slower than that of the lamellar compositions.

To be able to determine what is driving the changes in polymerization rate in the DTAB/water/PEG-400-DMA system, the propagation and termination parameters were again determined. In Figure 10, the rate parameters of propagation and termination are plotted as a function of conversion of double bonds for the 35 and 70 wt % DTAB compositions, corresponding to an isotropic micellar and lamellar mesophase, respectively.

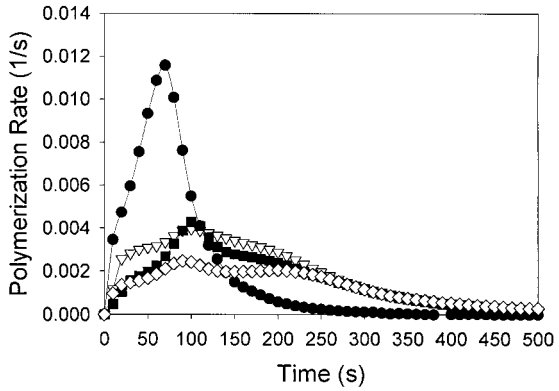

Figure 10. Polymerization rate vs time for 20% HEMA in the LLC phases of DTAB/water. Shown are 40% isotropic (◇), 45% cubic (■), 55% hexagonal (▽), and 65% lamellar (●) DTAB.

For both mesophases the propagation rate parameter k_p remains essentially the same for all conversions. However, an order of magnitude decrease in k_t is observed in the lamellar sample that polymerized $2^1/_2$ times faster than that of the isotropic micellar sample. Such a decrease in k_t indicates a decrease in the rate of termination, thereby yielding more propagating radicals and giving an overall faster polymerization rate. This behavior appears to be due to the more ordered nature of the lamellar mesophase. Similar results are also observed in the polymerization of small concentrations of certain monomers in thermotropic liquid crystalline systems.[8] In more ordered liquid crystalline phases faster polymerization rates are seen due to suppression of termination brought about by diffusional limitations of the propagating polymer chains.[8] Almost identical kinetic results are observed for a polymerizable amphiphile with the polymerizable double bond located near the polar headgroup.[20] The depression of k_t may indicate that the PEG-400-DMA is closely associated with the interface as opposed to being completely solubilized in the water domains of the LLC. Interestingly, other studies have shown that hydrophobically modified poly(ethylene glycol) aggregate with cationic surfactants quite readily.[33]

To determine whether the monomers were freely solvated or aggregated with the DTAB, ^{13}C spin−lattice T_1 relaxation times were determined for the carbons of PEG-400-DMA solvated in D_2O without surfactant and in micellar solutions of DTAB. Table 1 shows the T_1 of various carbons of the PEG-400-DMA in D_2O and that of the micellar solutions consisting of DTAB, PEG-400-DMA, and D_2O. The T_1's for the isotropic PEG-400-DMA are significantly higher in the isotropic state as compared to the micellar solutions. For example, the T_1 of the carbonyl carbon exhibits a 25% decrease from the isotropic to the micellar state. The vinyl carbons and the methyl carbons T_1 show a similar decrease when in the micellar phase. The ether carbons exhibit approximately a 10% decrease in T_1 in the micellar phase. In the solution state higher T_1's indicate faster motions which means the monomer in the micellar solution is experiencing a much more constrained environment. The polar PEG-400-DMA therefore appears to be aggregating with DTAB and is not exclusively segregated in the water domains.

Similar kinetic experiments were performed for the monofunctional polar monomer HEMA. HEMA exhibits very similar polymerization behavior to that of the PEG-400-DMA with the LLC morphology actually appearing

Table 1. ^{13}C Spin−Lattice Relaxation Times for the Carbons of PEG-400-DMA

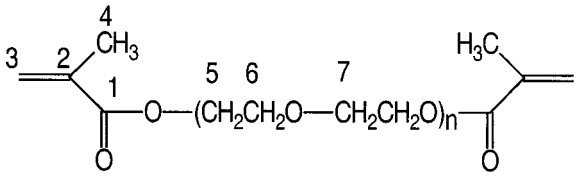

PEG-400-DMA

* (Relative Standard Error is less than 7%)

	0% DTAB isotropic	30% DTAB micellar
1	7.1	5.3
2	7.7	5.8
3	0.48	0.35
4	2.5	1.7
5	0.45	0.40
6	0.47	0.39
7	0.43	0.37

to have an even greater impact. In Figure 10 the polymerization rate profiles of 20% HEMA in the various LLC phases of DTAB/water is displayed. Similar to PEG-400-DMA and in contrast to the nonpolar monomers HDDA and *n*-DA, the fastest polymerization rates for HEMA are observed in the lamellar mesophase at 60 wt % DTAB. When the DTAB concentration is reduced in concentration to a hexagonal phase, the polymerization rate decreases by a factor of 3. The discontinuous cubic phase exhibits a similar polymerization rate to that of the hexagonal phase. The features of the polymerization rate profiles are different for the cubic mesophase and the hexagonal phase as compared to the lamellar sample. For example, the peak rate is reached at a later time than that of the lamellar polymerization, and the polymerizations actually accelerate later in the course of the reaction for both the cubic and hexagonal phases. The polymerization rate of 20% HEMA in the isotropic micellar phase consisting of 40 wt % DTAB decreased to a minimum that is approximately 4 times less when compared to the lamellar polymerization. This kinetic phenomenon is a consequence of increased LLC order that lowers the termination rate to yield the faster polymerization rates.

To be able to successfully generate polymeric materials with nanometer size morphologies, it is important not only to understand the polymerization behavior but also to develop an understanding of the structural evolution of the polymer. It is of great importance to determine whether the original phase is retained upon polymerization. To determine how the original lyotropic liquid crystalline order changes in response to the polymerization, polarized light microscopy was used to observe the textures before and after polymerization. Figure 11 depicts the cured and uncured hexagonal and lamellar phases containing 10 wt % HDDA in DTAB/water. In the case of the sample containing 70 wt % DTAB, the PLM micrograph exhibits maltese cross and "oily streak" textures that are indicative of the lamellar mesophase. Upon photopolymerization of the lamellar sample the texture changes to a pattern that is readily identified as lamellar as well. Interestingly, no gross phase separation is observed upon polymerization, indicating that the original LLC structure is retained to a large degree. The 50 wt % DTAB sample exhibits focal conic textures prior to polymerization that are indicative of the hexagonal mesophase. After polymer-

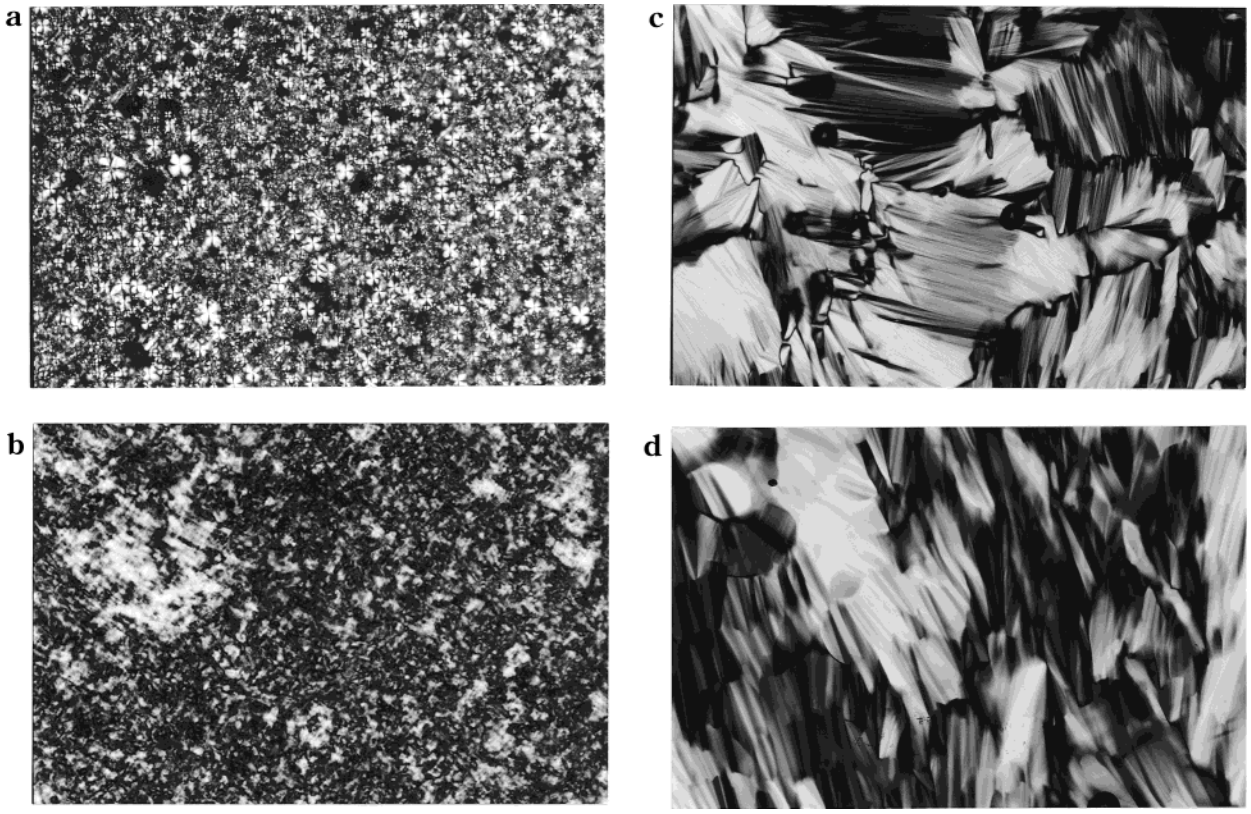

Figure 11. Polarized light micrographs of 10% HDDA in various compositions of DTAB/water before and after polymerization. Shown are (a) unpolymerized 70% DTAB-lamellar, (b) polymerized 70% DTAB-lamellar, (c) unpolymerized 50% DTAB-hexagonal, and (d) polymerized 50% DTAB-hexagonal.

ization the sample remains highly birefringent with retention of the focal conic textures. The textures of the polymerized hexagonal sample also appear slightly coarsened and subtly different, indicating that the nanostructure may be changing slightly upon polymerization. Despite these small differences, no gross phase separation is apparent upon cure, which implies that the original LLC structure is being retained to a great extent.

Similar experiments were performed on lamellar and hexagonal LLCs containing 20% PEG-400-DMA. As can be seen in Figure 12, the slower polymerizing hexagonal sample possesses textbook focal conic textures prior to polymerization. Upon complete cure the textures become less sharp, but the sample remains highly birefringent with no gross phase separation. The lamellar sample exhibits the typical mottled texture consisting of oily streaks and maltese crosses before polymerization. When the lamellar LLC is polymerized, the textures change very little with no apparent phase separation occurring. Again, the original lyotropic structure is being retained.

The possibility does exist for the LLC mixtures to phase separate on a microscopic scale that is undetectable with PLM. Initial work has been performed with SAXS to determine how the structures of these LLC systems change upon polymerization. In Figure 13 SAXS profiles of the hexagonal phase containing 10% HDDA is depicted in the uncured and cured state. The uncured profile has a primary reflection that corresponds to 34.7 Å and is very sharp, indicating a highly ordered LLC phase. Additionally, a weaker peak is observed at higher scattering angle corresponding to 20.1 Å The ratio of these two peaks is $1:1/3^{1/2}$, which is indicative of a hexagonal phase.[3] Upon polymerization there is little change in this profile. The primary peak of the cured sample does exhibit a slight shift to a higher scattering angle which corresponds to a smaller *d* spacing of 34.5 Å. A similar shift in the peak at higher scattering angle occurred, which yielded a *d* spacing of 19.9 Å. This pattern still is indicative of the hexagonal phase. This slight decrease in *d* spacing could be due to the typical volume contraction involved in vinyl polymerization. It appears that for these initial results the LLC structure is being templated successfully. Interestingly, the LLC may become more ordered upon polymerization as the primary reflection appears qualitatively to be more intense and narrower. Future work will explore in more detail the structure retention of the LLC phase in the polymeric materials.

Conclusions

The segregation behavior and polymerization kinetics of monomers with different polarities and chemical structure in surfactant/water lyotropic liquid crystal (LLC) systems are significantly different depending on the LLC morphology. Nonpolar monomers such as hexanediol diacrylate and *n*-decyl acrylate partition to the oil-soluble domains of the LLC, whereas the more polar monomers poly(ethylene glycol)-400-dimethacrylate and 2-hydroxyethyl methacrylate segregate at the water/liquid crystal interface. The polymerization kinetics in both cases are heavily dependent on the LLC morphologies but in opposite ways. The nonpolar monomers exhibit much faster polymerization rates in micellar aggregates than in hexagonal or lamellar phases. This behavior is a result of an apparent increase in the rate of propagation and termination induced by higher local concentrations of monomer in the micelles as compared to the other mesophases with more surfac-

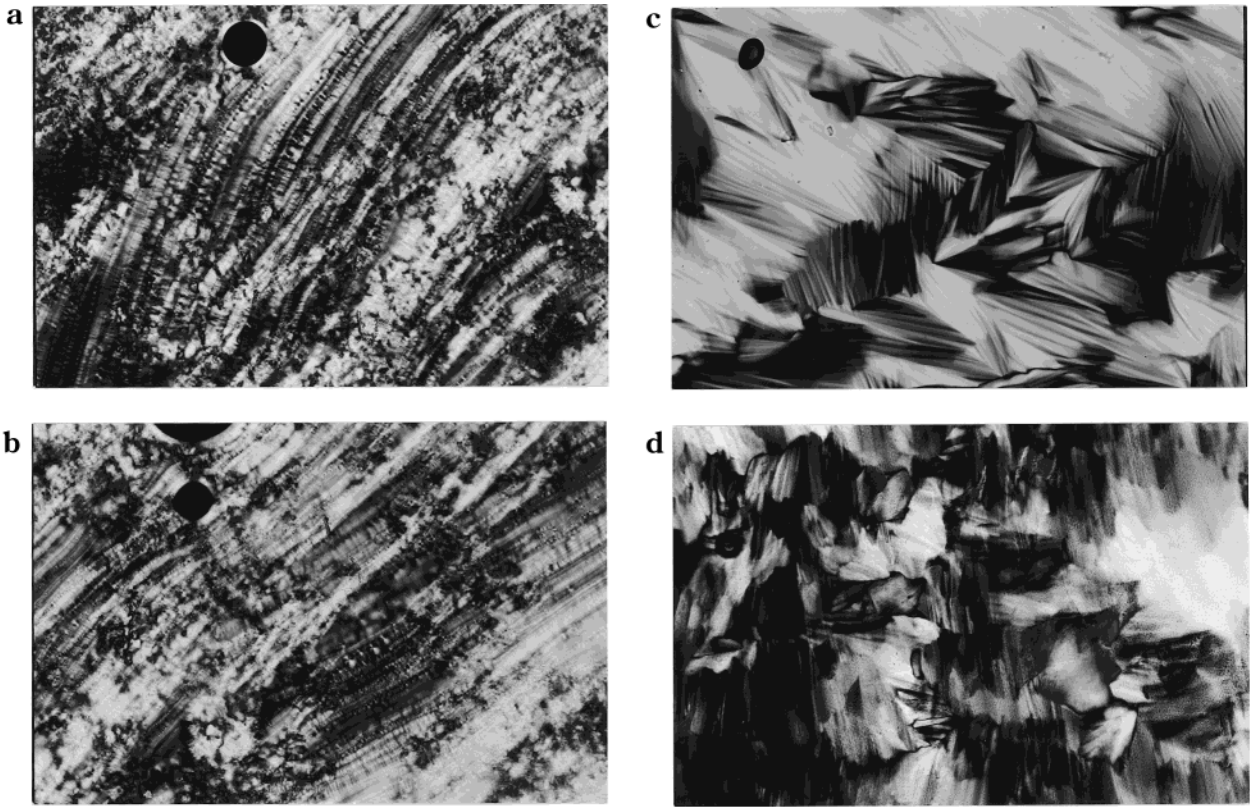

Figure 12. Polarized light micrographs of 20% PEG-400-DMA in various compositions of DTAB/water before and after polymerization. Shown are (a) unpolymerized 70% DTAB-lamellar, (b) polymerized 70% DTAB-lamellar, (c) unpolymerized 50% DTAB-hexagonal, and (d) polymerized 50% DTAB-hexagonal.

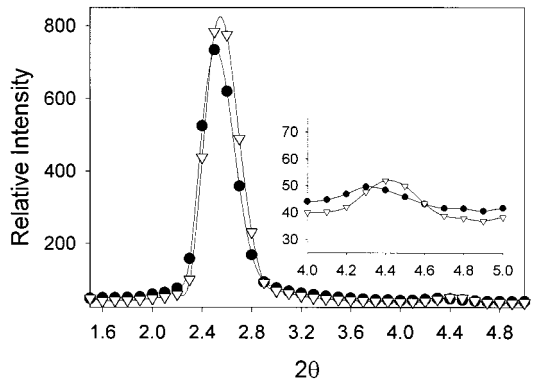

Figure 13. SAXS profiles of 10% HDDA in the hexagonal phase of 50% DTAB/water shown unpolymerized (●) and polymerized (▽).

tant. For more polar monomers the opposite behavior is observed. The fastest polymerizations occur in the highly ordered lamellar mesophase. The polymerization rates reach a minimum in the isotropic micellar phase. In this case the enhanced polymerization rates are a consequence of depressed termination rates in the lamellar mesophases. The depressed termination rates in the lamellar mesophase are a result of diffusional limitations imposed by the high degree of order on the propagating polymer chains. NMR results indicate that the polar monomers are aggregating with the surfactant in the LLC phases which explains the dependence of these monomers on the degree and type of LLC order. Initial results also indicate that the original LLC phase morphologies are retained upon photopolymerization. In summary, templated photopolymerizations of organic monomers of different chemical nature exhibit drastically different polymerization kinetics with different LLC morphologies. This behavior has significant implications on the resulting polymer morphology and ultimate structure retention.

Acknowledgment. The authors thank the University of Southern Mississippi, Petroleum Research Fund, and the National Science Foundation (CTS-0093911) for financial support of this project.

References and Notes

(1) Antonietti, M.; Hentze, H. P. *Colloid Polym. Sci.* **1996**, *274*, 696.
(2) Antonietti, M.; Caruso, R. A.; Göltner, C. G.; Weissenberger, M. C. *Macromolecules* **1999**, *32*, 1383.
(3) Gray, G. W.; Winsor, P. A. *Liquid Crystals & Plastic Crystals*, 1st ed.; Gray, G. W., Winsor, P. A., Eds.; John Wiley & Sons: New York, 1974; Vol. 1, p 314.
(4) Kelker, H.; Hatz, R. *Handbook of Liquid Crystals*, 1st ed.; Verlag Chemie: Weinheim, 1980.
(5) Paleos, C. M. *Polymerization in Organized Media*; Paleos, C. M., Ed.; Gordon and Breach Science Publishers: Philadelphia, 1992; p 183.
(6) Guymon, C. A.; Bowman, C. N. *Macromolecules* **1997**, *30*, 1594.
(7) Guymon, C. A.; Hoggan, N. A.; Rieker, T. P.; Walba, D. M.; Bowman, C. N. *Science* **1997**, *275*, 57.
(8) Guymon, C. A.; Bowman, C. N. *Macromolecules* **1997**, *30*, 5271.
(9) Guymon, C. A.; Dougan, L. A.; Martens, P. J.; Clark, N. A.; Walba, D. M.; Bowman, C. N. *Chem. Mater.* **1998**, *10*, 2378.
(10) McGrath, K. M. *Colloid Polym. Sci.* **1996**, *274*, 499.
(11) McGrath, K. M.; Drummond, C. J. *Colloid Polym. Sci.* **1996**, *274*, 316.
(12) McGrath, K. M.; Drummond, C. J. *Colloid Polym. Sci.* **1996**, *274*, 612.
(13) McGrath, K. M. *Colloid Polym. Sci.* **1996**, *274*, 399.
(14) Thundathil, R.; Stoffer, J. O. *J. Polym. Sci., Polym. Chem. Ed.* **1980**, *18*, 2629.
(15) Srisiri, W.; Sisson, T. M.; O'Brien, D. F.; McGrath, K. M.; Han, Y. S.; Gruner, S. M. *J. Am. Chem. Soc.* **1997**, *119*, 4866.

(16) Lee, Y. S.; Yang, J. Z.; Sisson, T. M.; Frankel, D. A.; Gleeson, J. T.; Aksay, E.; Keller, S. L.; Gruner, S. M.; O'Brien, D. F. *J. Am. Chem. Soc.* **1995**, *117*, 5573.
(17) Gray, D. H.; Gin, D. L. *Chem. Mater.* **1998**, *10*.
(18) Deng, H.; Gin, D. L.; Smith, R. C. *J. Am. Chem. Soc.* **1998**, *120*, 3522.
(19) Smith, R. C.; Fischer, W. M.; Gin, D. L. *J. Am. Chem. Soc.* **1997**, *119*, 4092.
(20) Lester, C. L.; Guymon, C. A. *Macromolecules* **2000**, *33*, 5448.
(21) Beck, J. S.; Vartuli, J. C.; Roth, W. J.; Leonowicz, M. E.; Kresge, C. T.; Schmitt, K. D.; Chu, C. T.-W.; Olson, D. H.; Sheppard, E. W.; McCullen, S. B.; Higgens, J. B.; Schlenker, J. L. *J. Am. Chem. Soc.* **1992**, *114*, 10834.
(22) Monnier, A.; Schuth, F.; Huo, Q.; Kumar, D.; Margolese, D.; Maxwell, R. S.; Stucky, G. D.; Krishnamurty, M.; Petroff, P.; Firouzi, A.; Janicke, M.; Chmelka, B. F. *Science* **1993**, *261*, 1299.
(23) Fyfe, C. A.; Fu, G. *J. Am. Chem. Soc.* **1995**, *117*, 9709.
(24) Tanev, P. T.; Pinnavaia, T. J. *Science* **1995**, *267*, 865.
(25) Firouzi, A.; Kumar, D.; Bull, L. M.; Besier, T.; Sieger, P.; Huo, Q.; Walker, S. A.; Zasadzinski, J. A.; Glinka, C.; Nicol, J.; Margolese, D.; Stucky, G. D.; Chmelka, B. F. *Science* **1995**, *267*, 1138.
(26) Huo, Q.; Leon, R.; Petroff, P. M.; Stucky, G. D. *Science* **1995**, *268*, 1324.
(27) Braun, P. V.; Osenar, P.; Tohver, V.; Kennedy, S. B.; Stupp, S. I. *J. Am. Chem. Soc.* **1999**, *121*, 7302.
(28) Anderson, D. M.; Strom, P. *Physica A* **1991**, *176*, 151.
(29) Li, T. D.; Gan, L. M.; Chew, C. H.; Teo, W. K.; Gan, L. H. *Langmuir* **1996**, *12*, 5863.
(30) Göltner, C. G.; Antonietti, M. *Adv. Mater.* **1997**, *9*, 431.
(31) Kroschwitz, J.; Mark, H.; Overberger, C.; Bikules, N.; Menges, G. *Encyclopedia of Polymer Science and Engineering;* Kroschwitz, J., Mark, H., Overberger, C., Bikules, N., Menges, G., Eds.; J. Wiley and Sons: New York, 1985; Vol. 1A.
(32) The sample consisting of 35 wt % DTAB, 55 wt % water, and 10 wt % PEG-400-DMA exhibited the most variability of all of the kinetic experiments. The relative standard error was calculated by dividing the standard deviation of the maximum polymerization rates from five identical experiments by the average of these experiments. The relative standard error was 3.5% for this particular composition, and all other maximum rates determined in this fashion exhibited less variability.
(33) Rubingh, D. N.; Holland, P. M. In *Cationic Surfactants: Physical Chemistry*; Rubingh, D. N., Holland, P. M., Eds.; Marcel Dekker: New York, 1991; Vol. 37.

MA001853E